Atmos. Chem. Phys., 24, 5479–5494, 2024
https://doi.org/10.5194/acp-24-5479-2024

Atmospheric Chemistry and Physics
Open Access
EGU

Contribution of fluorescent primary biological aerosol particles to low-level Arctic cloud residuals

Gabriel Pereira Freitas[1,2], Ben Kopec[3], Kouji Adachi[4], Radovan Krejci[1,2], Dominic Heslin-Rees[1,2], Karl Espen Yttri[5], Alun Hubbard[6,7], Jeffrey M. Welker[8,9,10], and Paul Zieger[1,2]

[1]Department of Environmental Science, Stockholm University, Stockholm, Sweden
[2]Bolin Centre for Climate Research, Stockholm University, Stockholm, Sweden
[3]Great Lakes Research Center, Michigan Technological University, Houghton, MI, USA
[4]Department of Atmosphere, Ocean, and Earth System Modeling Research, Meteorological Research Institute, Tsukuba, Japan
[5]The Climate and Environmental Research Institute NILU, Kjeller, Norway
[6]The Centre for Ice, Cryosphere, Carbon and Climate, Institutt for Geovitenskap, UiT – The Arctic University of Norway, Tromsø, Norway
[7]Geography Research Unit, University of Oulu, Oulu, Finland
[8]Department of Biological Sciences, University of Alaska Anchorage, Anchorage, AK, USA
[9]University of the Arctic, Rovaniemi, Finland
[10]Ecology and Genetics Research Unit, University of Oulu, Oulu, Finland

Correspondence: Paul Zieger (paul.zieger@aces.su.se)

Received: 3 November 2023 – Discussion started: 5 December 2023
Revised: 23 March 2024 – Accepted: 27 March 2024 – Published: 13 May 2024

Abstract. Mixed-phase clouds (MPCs) are key players in the Arctic climate system due to their role in modulating solar and terrestrial radiation. Such radiative interactions rely, among other factors, on the ice content of MPCs, which is regulated by the availability of ice-nucleating particles (INPs). While it appears that INPs are associated with the presence of primary biological aerosol particles (PBAPs) in the Arctic, the nuances of the processes and patterns of INPs and their association with clouds and moisture sources have not been resolved. Here, we investigated for a full year the abundance of and variability in fluorescent PBAPs (fPBAPs) within cloud residuals, directly sampled by a multiparameter bioaerosol spectrometer coupled to a ground-based counterflow virtual impactor inlet at the Zeppelin Observatory (475 m a.s.l.) in Ny-Ålesund, Svalbard. fPBAP concentrations (10^{-3}–10^{-2} L^{-1}) and contributions to coarse-mode cloud residuals (0.1 to 1 in every 10^3 particles) were found to be close to those expected for high-temperature INPs. Transmission electron microscopy confirmed the presence of PBAPs, most likely bacteria, within one cloud residual sample. Seasonally, our results reveal an elevated presence of fPBAPs within cloud residuals in summer. Parallel water vapor isotope measurements point towards a link between summer clouds and regionally sourced air masses. Low-level MPCs were predominantly observed at the beginning and end of summer, and one explanation for their presence is the existence of high-temperature INPs. In this study, we present direct observational evidence that fPBAPs may play an important role in determining the phase of low-level Arctic clouds. These findings have potential implications for the future description of sources of ice nuclei given ongoing changes in the hydrological and biogeochemical cycles that will influence the PBAP flux in and towards the Arctic.

1 Introduction

Mixed-phase clouds (MPCs) contain both cloud droplets and ice crystals (Korolev et al., 2003). Their interaction with solar and terrestrial radiation depends on their ice-to-droplet ratio, altitude, thickness, and other factors (Matus and L'Ecuyer, 2017). The phase of an MPC can be affected by the aerosol population in the cloud (Storelvmo, 2017), especially by the presence of particles that can facilitate the formation of ice: the ice-nucleating particles (INPs; see, e.g., Kanji et al., 2017). Therefore, a key element in an improved understanding of MPCs in the Arctic is unraveling the sources, properties, and concentrations of INPs (Solomon et al., 2018).

The representation of MPCs and other aerosol–cloud interactions comprises important sources of uncertainties in climate models, impacting our ability to correctly estimate radiative forcing in the Earth's climate system (Szopa et al., 2021). This is especially true in remote regions, such as the Arctic, where measurements are scarce (Schmale et al., 2021) and low-level MPCs are prevalent throughout the year (Kay et al., 2016; Morrison et al., 2012). The Arctic has experienced surface temperature increases that are 2 to 4 times higher than the global average (Rantanen et al., 2022), a phenomenon known as Arctic amplification (Wendisch et al., 2023). Clouds are believed to be a key contributor to the Arctic radiative budget, prompting the need to improve our understanding of aerosol–cloud interactions in the Arctic (Schmale et al., 2021).

INPs facilitate ice growth at temperatures above that of homogeneous nucleation (i.e., temperatures below $-38\,^{\circ}\mathrm{C}$) (Kanji et al., 2017). Complete or partial glaciation of a cloud radically changes its radiative properties and lifetime and can even trigger precipitation (Lensky and Rosenfeld, 2003; Stopelli et al., 2015). In the Arctic, high-temperature INPs have been observed on a seasonal basis (Porter et al., 2022; Sze et al., 2023) and have been linked to biogenic, oceanic, and terrestrial sources (Creamean et al., 2018; Šantl-Temkiv et al., 2019; Hartmann et al., 2020; Creamean et al., 2022; Pereira Freitas et al., 2023) along with dust emissions (Tobo et al., 2019). Satellite observations show that the prevalence of MPCs in the Arctic and Antarctic regions can be explained to a large degree by the presence of INPs (Carlsen and David, 2022). Despite satellite remote sensing uncertainties, their results reflect those of ground-based remote sensing in the Arctic (Nomokonova et al., 2019).

Primary biological aerosol particles (PBAPs) are biological particles that are emitted directly from the source to the atmosphere. These can be, but are not limited to, microorganisms, biological functional parts, fungal spores, or fragments of vegetation (Després et al., 2012; Fröhlich-Nowoisky et al., 2016). Some PBAPs are efficient INPs, even at high temperatures ($> -15\,^{\circ}\mathrm{C}$; Tobo et al., 2013). This is due to their microphysical properties and/or their excretion of ice-nucleating proteins (Pummer et al., 2015). In the Arctic, PBAPs dominate the number of high-temperature INPs in summer (Sze et al., 2023; Pereira Freitas et al., 2023).

Some PBAPs, such as bacteria, have been observed in cloud water samples and showed cloud condensation (Bauer et al., 2002, 2003) and ice-nucleating abilities (Joly et al., 2013). These in-cloud bacteria undergo cloud processing (Khaled et al., 2021), reproduction, and growth (Sattler et al., 2001). Offline methods used to sample PBAPs are limited in quantifying their abundance (Huffman et al., 2020). To overcome such limitations, online methods can be used, such as those based on single-particle ultraviolet laser-induced fluorescence (Huffman et al., 2020), which has been shown to give reasonable estimates of PBAP concentration in real time (Freitas et al., 2022; Crawford et al., 2017, 2020). Given the close link between PBAPs and high-temperature INPs (Šantl-Temkiv et al., 2019; Creamean et al., 2019; Pereira Freitas et al., 2023), obtaining PBAP concentrations inside cloud particles is one way to understand the impact of PBAPs serving as INPs in cloud glaciation.

The ground-based counterflow virtual impactor (CVI) has been successfully used in recent years to improve our process-level understanding of aerosol–cloud interactions in the Arctic, for example, by determining the size distributions (of sub-micrometer aerosol; Karlsson et al., 2021, 2022), the chemical composition (Gramlich et al., 2023), or the black carbon concentration (Zieger et al., 2023) of cloud residuals, i.e., particles which were involved in cloud formation or cloud processes. In this study, we present the first investigation of the contribution of PBAPs to cloud residuals in the Arctic.

Some studies evaluated the sources of INPs and PBAPs using back trajectories (Si et al., 2019; Meinander et al., 2022; Shi et al., 2022; Creamean et al., 2022; Pereira Freitas et al., 2023). Another method to investigate the air origin is to use the water isotope ratios (hydrogen, δD, and oxygen, $\delta^{18}\mathrm{O}$), which have been used to distinguish regional and transported sources of air (Sodemann et al., 2008; Sjostrom and Welker, 2009; Bonne et al., 2015; Noone et al., 2011). This determination of source and transport history is possible because isotope ratios in water vapor and precipitation are largely controlled by the conditions at the point of evaporation, which change as the air mass is carried over the atmosphere (Merlivat and Jouzel, 1979; Xia et al., 2022). In the Arctic, water isotopic measurements have been used to distinguish between moisture sourced regionally in response to variations in sea ice coverage and moisture sourced from distant locations (Kopec et al., 2016; Bonne et al., 2019; Akers et al., 2020; Bailey et al., 2021). In Svalbard, it has been shown that low deuterium ($^{2}\mathrm{H}$) excess values ($< 5\,‰$) are typically driven by air masses comprised of predominantly regionally sourced moisture, while high values ($> 10\,‰$) are found in air masses comprised of predominantly distantly sourced moisture (Kopec et al., 2016). Pairing CVI sampling of cloud particles with water vapor isotopic measurements

can improve understanding of the origin of a given air mass and aid in the source identification of INPs and PBAPs.

We investigate the presence and impact of PBAPs in low-level Arctic clouds present at the Zeppelin Observatory in Svalbard and address the following research questions: (i) can we identify PBAPs within cloud particles of low-level Arctic clouds using an online single-particle instrument coupled to a CVI inlet? (ii) If so, to what extent are they present throughout the year and what are their respective sources? And finally, (iii) if present, can we identify an impact on the cloud phase?

2 Methods

2.1 Campaign description

The measurements were part of the Ny-Ålesund Aerosol Cloud Experiment (NASCENT) 2019–2020 campaign. A complete overview of the campaign is given by Pasquier et al. (2022). In short, for 1.5 years, which coincided with the MOSAiC expedition in the central Arctic (Shupe et al., 2022), several state-of-the-art aerosol, cloud, and meteorological measurements from different platforms were taken concurrently at various locations around Ny-Ålesund in a combined effort to unravel the properties of clouds and aerosols in the Arctic. In this work, we focus on measurements taken at the Zeppelin Observatory, which is located 475 m above sea level (a.s.l.) close to the top of the Zeppelin mountain, 2 km south of the village. Due to the topography of the mountain, the wind tends to blow predominantly from the south or from the north, with very little influence from crosswinds (see, e.g., Pasquier et al., 2022). The observatory was engulfed in low-level clouds for 34 % of the campaign duration (visibility below 1 km as measured by the visibility sensor; see Sect. 2.2). The entire setup is illustrated in Fig. 1.

2.2 Cloud particle sampling

Cloud droplets and ice crystals were collected using a ground-based counterflow virtual impactor (CVI) inlet (model 1205, Brechtel Manufacturing Inc., USA). The CVI only collects particles above approx. 6 µm in aerodynamic diameter, representing aerosol particles that have been activated in cloud droplets or ice crystals. It does so by accelerating the cloud onto the CVI tip that is installed within a wind tunnel. Within the CVI tip, a counterflow is targeted against the sample flow where only larger particles have enough inertia to penetrate through the virtual impaction plate. A more technical description of the CVI is given in Noone et al. (1988) and Shingler et al. (2012), whereas a detailed characterization of the ground-based CVI present at the Zeppelin Observatory, together with the applied corrections, is given in Karlsson et al. (2021). After the cloud droplets and ice crystal penetrate through the virtual impaction plate, they are dried in the counterflow air. The leftover nuclei are called cloud residuals, which are then sampled by the aerosol instrumentation downstream of the CVI. The measured cloud residual concentration after correcting for an enrichment factor (9.8 for this work) must be multiplied by a factor of 2, accounting for a mean droplet sampling efficiency of around 45 %. This factor was determined by comparing the coarse-mode cloud residual particle concentration (> 0.8 µm) measured by the multiparameter bioaerosol spectrometer (MBS) during CVI operation with the corresponding ambient (total) coarse-mode particle concentration measured by a Fidas 200 S (Palas GmbH, Germany) sampling from its own inlet located on the terrace of the Zeppelin Observatory (see Fig. S1 in the Supplement). This value is comparable to the CVI sampling efficiency of 46 % previously determined by Karlsson et al. (2021).

A visibility sensor was coupled to the CVI inlet (model 6400, Belfort Instrument, USA). Whenever the visibility falls below 1000 m, indicating the presence of clouds according to the World Meteorological Organization (WMO) (Spänkuch et al., 2022; WMO, 2008), the CVI inlet is meant to be turned on. For part of the observational period of this study, the CVI was turned on automatically. However, it was turned on manually for certain periods due to severe icing conditions. Given the manual operation of the CVI inlet and fluctuation in visibility to values above 1 km (leading to a short automatic stop of the CVI inlet sampling) within a short period, several cloud events (CEs) could be contained within a single cloud, and some clouds were not sampled at all. Despite our best efforts to obtain a balanced dataset throughout all seasons, the issues with icing on the inlet during cold periods with supercooled liquid cloud droplets led to fewer samples in the winter months. It should be noted that the summer generally shows denser clouds with a higher cloud water content and lower visibilities during cloudy conditions (see Fig. S6 in Zieger et al., 2023). Nonetheless, there are several CEs successfully sampled during winter, thus covering all months of the year. The exception is April 2020, when the MBS did not function. An overview of the CEs sampled is given in Table S1 (in the Supplement). The first minute of every CE was discarded to remove possible contamination by particles remaining in the inlet from previous sampling and switching of the inlet.

2.3 Single-particle bioaerosol characterization

The single-particle characterization of the cloud residuals was performed using a multiparameter bioaerosol spectrometer (MBS, University of Hertfordshire, UK). The MBS is a single-particle instrument based on laser-induced fluorescence (Ruske et al., 2017). In summary, a laminar sample flow ($0.315\,\mathrm{L\,min^{-1}}$) shielded by a sheath flow ($1.715\,\mathrm{L\,min^{-1}}$, summing up to $2.03\,\mathrm{L\,min^{-1}}$ of total flow) guides particles through the instrument. A continuous low-power laser light is scattered by particles, and their size is retrieved by the intensity of the scattered light. Then, a xenon

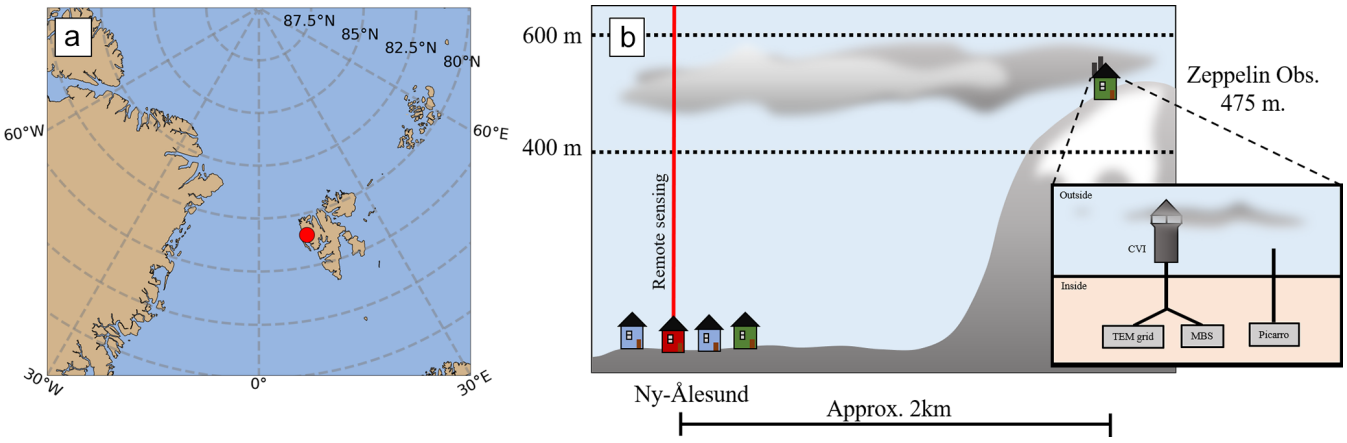

Figure 1. Sampling location and measurement setup. **(a)** Location of Ny-Ålesund on the Norwegian archipelago of Svalbard (red dot). **(b)** Schematic demonstrating the positioning of the different measurements in the town of Ny-Ålesund, where remote sensing took place, and at the Zeppelin Observatory (475 m a.s.l.), where in situ cloud, aerosol, and water vapor measurements were performed. For the cloud characterization via Cloudnet, the altitude between 400 and 600 m was taken into account (dashed line). At the Zeppelin Observatory, the transmission electron microscopy (TEM) grid sampler and the multiparameter bioaerosol spectrometer (MBS) sampled cloud residuals from a counterflow virtual impactor (CVI) inlet. The Picarro analyzer sampled water vapor from its own gas-phase inlet.

flashlamp is triggered, shining at the particle with a 280 nm ultraviolet light. The instrument can reliably measure the fluorescence of particles with an optical diameter of 0.8 µm or larger. If the particle fluoresces, its emitted light is collected by two collection mirrors and focused onto a diffraction grating. The diffracted light is then focused onto a detector covering the visible range between the wavelengths of 300–615 nm over eight equally distant channels. Following the previous work by Freitas et al. (2022), if the fluorescence is more than 9 times the fluorescence background and its main signal sits at 364 nm (tryptophan emission channel, a common protein in microorganisms; see, e.g., Pöhlker et al., 2012), the particle is classified as a fluorescent primary biological aerosol particle (fPBAP). A general drawback of these methods is uncertainty relating to over-counting (fluorescent particles erroneously classified as PBAPs) and under-counting (potential non-fluorescent PBAPs not being counted).

2.4 Water vapor isotope measurements

Continuous atmospheric water vapor isotopic measurements accompanied the CVI inlet sampling at the Zeppelin Observatory to assist in source identification of water vapor and air mass history. Water vapor concentration and isotopic ratios of oxygen ($\delta^{18}O$) and hydrogen (δD) were measured using a Picarro L2130-i isotope and gas concentration analyzer (Picarro, Inc., USA). Deuterium excess (d-excess) values were computed in the form of $d = \delta D - 8 \times \delta^{18}O$ (Dansgaard, 2012). The Picarro analyzer was also located in the Zeppelin Observatory (Fig. 1). Inlet tubing (≈ 3 m in length) sampled ambient air directly above the roof of the laboratory building a few meters from the CVI. Isotopic observations began on 14 November 2019 and continued through the end of December 2020 to overlap with most of the cloud observation window.

To calibrate the water vapor isotopic measurements, the Picarro analyzer is connected to a Picarro Standards Delivery Module (SDM). Data calibration and processing for the measurements at the Zeppelin Observatory follow those made at Pallas, Finland, using a similar instrument (Bailey et al., 2021). Every ≈ 24 h, the SDM supplied two water samples of known isotopic composition that bracketed the range of isotopic measurements to standardize the measurements. The two standards used were USGS45 ($\delta^{18}O = -2.238$ ‰, $\delta D = -10.3$ ‰) and USGS49 ($\delta^{18}O = -50.55$ ‰, $\delta D = -394.7$ ‰). These standards were used to correct for any offsets to the VSMOW–SLAP scale and assess any instrument drift, which was minimal during the measurement period. Given the low water vapor concentration at times during this measurement period (< 1000 ppm), it is necessary to correct any instrument bias that might exist at these lower concentrations (Steen-Larsen et al., 2013). A humidity experiment was carried out at the time of the installation of the instrument and followed the protocol described by Akers et al. (2020) that included the measurement of the two standard waters over a range of water vapor concentrations regulated by dry air. A humidity response curve was developed and applied to the dataset. Additional data quality control protocols followed the methods described by Bailey et al. (2021). Once quality control and calibrations were conducted, water vapor concentration and isotopic ratios ($\delta^{18}O$, δD, d-excess) were aggregated into 5 min averages. The data were further aggregated to only times when the CVI was sampling to appropriately pair the isotopic observations with a given CE. Given the instrument

analytical error and error in the calibration process, we estimate uncertainty to be $< 0.3\,‰$ for $\delta^{18}O$, $< 1.1\,‰$ for δD, and $< 2.1\,‰$ for d-excess. Error values are highest when water vapor concentration is lowest. However, for the purpose of this analysis, we only focused on times when clouds were present, which are related to times of relatively higher water vapor content; thus, the uncertainty in the isotopic measurements is generally lower than it would be across the entire dataset. Importantly, these instrument- and analysis-based errors are significantly lower than the natural variability explored in this study.

2.5 Cloud type classification

Unlike in situ cloud sampling at the Zeppelin Observatory, the Cloudnet dataset was retrieved for the region around the village of Ny-Ålesund approx. 2 km away from the observatory (Nomokonova et al., 2019). Using a combination of remote sensing techniques, a vertically resolved cloud classification of the air column is obtained (Illingworth et al., 2007). This classification is explained in depth for Ny-Ålesund in Nomokonova et al. (2019, 2020). In short, at 20 m intervals, the air column is classified according to its physical properties. This covers clear sky (CS), cloud droplets (CD), drizzle (DR), cloud droplets and drizzle (DR + CD), ice crystals (I), ice crystals and supercooled droplets (I + SCD), melting ice (MI), melting ice and cloud droplets (MI + CD), aerosol (A), insects (Ins), and aerosol and insects (A + Ins). Here, we analyze altitudes of 400 to 600 m to reflect measurements taken at the Zeppelin Observatory altitude (475 m a.s.l.). Potential problems this approach poses to cloud classification could include cases where the cloud over Ny-Ålesund might not be the same as that at the Zeppelin mountain or where a cloud is present at one site and not at the other. However, given the long sampling times (longer than 30 min), there is a good chance that the cloud would be present at both sites for at least a portion of the sampling time, which is sufficient for CE classification. Table S1 describes all CEs and the availability of Cloudnet data.

For each CE, an ice-to-droplet ratio is derived using the Cloudnet dataset. As previously done in Karlsson et al. (2021), this value is calculated as the ratio of ice-related classification points (I, I + SCD, MI, and MI + CD) to droplet-related classification points (CD, DR, and CD + DR). For those CEs with a ratio between ice and liquid classifications ($> 10\,\%$ and $< 90\,\%$), a mixed-phase cloud (MPC) classification is given. The Cloudnet data also provide the height of the cloud top (Chellini et al., 2022), but we have chosen to manually assess the lowest-level cloud top height based on the column profile.

2.6 Auxiliary parameters

The ambient air temperature and relative humidity (at the Zeppelin Observatory) were measured by a weather station coupled to the CVI. Furthermore, the column air temperature was recovered from daily radio soundings taken in the village of Ny-Ålesund (Maturilli, 2020) and using the Humidity and Temperature Profiler (HATPRO) sensor located at the AWIPEV station (Rose et al., 2005). These air temperature curves were used to recover the height at which the air temperature reached −15 °C in a daily (radio soundings) and per CE (HATPRO) resolution.

For one CE in September 2020, a coarse-mode aerosol sample grid used for transmission electronic microscopy (TEM; for particles above 0.7 µm in aerodynamic diameter) successfully sampled cloud residuals for 30 min at 1 L min^{-1} downstream of the CVI inlet and the particles were classified using the elemental composition described by Adachi et al. (2022).

2.7 Back trajectory analysis

Back trajectory ensembles were initialized at a height of 250 m at the latitude and longitude of the observatory, every hour for the days in which there were valid observations. The ensemble was generated by shifting the meteorological fields whilst keeping the initialized starting point the same; in total, 27 back trajectories were initialized in each ensemble. The length of the back trajectories was restricted to 5 d. Data points along each and every back trajectory (i.e., endpoints) were selected only if they resided within the mixed layer (as defined by the model/HYSPLIT output). Previous work by Karlsson et al. (2021) showed that increasing or decreasing the mixing layer height does not significantly affect the general contribution of surface types. The endpoints were temporally and spatially collocated with gridded sea ice daily data derived from satellite observations (Copernicus Climate Change Service, 2020) to ascertain the surface type directly below each endpoint, within the mixed layer. All back trajectories were carried out using the HYSPLIT V5.2.1 model (Draxler et al., 1998; Stein et al., 2015), with the Global Data Assimilation System (GDAS) $1° \times 1°$ archive data used for the metrological fields (https://www.ready.noaa.gov/data/archives/gdas1/, last access: 12 July 2023). The Python package PySPLIT (Cross, 2015) was used to generate the ensemble back trajectories.

3 Results and discussion

We collected 209 CEs of at least 30 min duration from June 2019 to December 2020. For each CE, the coarse-mode cloud residuals (optical diameter > 0.8 µm) were characterized in a single-particle manner by the MBS, resolving the fPBAP contribution for each CE.

First, we present an overview of fPBAPs found in cloud residuals (Sect. 3.1 and 3.2). Second, we include an analysis of the annual cycle of all characterized CEs (Sect. 3.3) and their source allocation (Sect. 3.4). Finally, we present a case study of a mixed-phase cloud event with the highest concentration of fPBAPs (Sect. 3.5). Similar case studies for a liquid-phase and an ice-phase cloud are briefly presented and discussed in Sect. S1.1 and S1.2 of the Supplement.

3.1 Characterization of fluorescent primary biological particles within cloud residuals

In total, 527 fPBAPs were detected by the MBS within cloud residuals (Table 1), accounting for less than 1 particle per cloud hour. In summer, fPBAP cloud residual concentrations ranged from 10^{-3}–$10^{-2}\,L^{-1}$ (mean: $8.1 \times 10^{-3}\,L^{-1}$), contributing up to 5 % (mean: 0.03 %) of the coarse-mode cloud residual particles. In winter, both the concentration and the relative contribution were lower (mean: $4.2 \times 10^{-3}\,L^{-1}$ and 0.005 %, respectively). These fPBAP concentrations are in the range of typical high-temperature INP concentrations found in the Arctic (10^{-4}–$10^{-1}\,L^{-1}$ at activation temperature ≈ -15 °C) (Creamean et al., 2022; Sze et al., 2023; Pereira Freitas et al., 2023). Of all sampled CEs in summer and winter, 67 % and 45 %, respectively, contained at least one fPBAP cloud residual. Despite PBAPs contributing significantly to the INP population in the Arctic (e.g., Pereira Freitas et al., 2023), they are not the only source (e.g., Tobo et al., 2019). Nonetheless, given the relatively high number of clouds containing fPBAPs and the susceptibility of Arctic clouds to having their phase modulated by low concentrations of INPs (Prenni et al., 2007), fPBAPs could be relevant in aiding cloud glaciation processes in Arctic low-level clouds.

3.2 Transmission electron microscopy of coarse-mode cloud residuals

For a CE on 22 September 2020, one TEM grid with identified PBAPs was successfully sampled for 30 min downstream of the CVI which overlapped with the MBS sampling. Using the elemental analysis described by Adachi et al. (2020, 2022), we assessed the probable nature of the coarse-mode cloud residuals sampled on the grid. The TEM images (Fig. 2a, b, and c) show 3 PBAPs that were part of cloud residuals (out of the 133 particles analyzed from the TEM grid or around 2 %). During the same CE, the MBS measured 5 fPBAP cloud residuals (Fig. 2d), accounting for 0.05 % of the total coarse-mode particles. Webcam images of the cloud are also shown in Fig. 2d. It should be noted that the cut sizes for the TEM grid and the MBS slightly differ (0.7 µm in aerodynamic and 0.8 µm in optical diameter, respectively). The d-excess for this CE was 0.3 ‰, which is a very low number, signaling that this cloud's water vapor was probably regionally sourced. Unfortunately, Cloudnet data were not available for this CE, so no assessment of the cloud phase could be made.

To the best of our knowledge, this is the first time PBAPs were directly imaged in cloud residuals (as opposed to being collected in a cloud water sample; Bauer et al., 2002), directly indicating their possible role as cloud condensation nuclei and/or INPs. However, it is difficult to draw further conclusions based on one sample; thus, this result should be taken as analysis supporting the more comprehensive MBS analysis.

3.3 Annual cycle of cloud parameters

Several parameters were averaged for each of the 209 CEs, including ambient temperature, d-excess, and ice-to-droplet ratio, which were subsequently grouped by month (Fig. 3). Above panel A of Fig. 3, the number of CEs (# cloud events) is shown along with the total hours sampled (# hours sampled) for each month of the year. As can be seen, most CEs were concentrated in summer, when sampling conditions were generally better. It is also documented that low-level clouds are also more present in the late summer (early fall) months (Illingworth et al., 2007; Taylor et al., 2019; Curry and Ebert, 1992; Maturilli and Ebell, 2018).

The concentration of coarse-mode aerosol particles within CEs was generally lower in summer and higher in winter months (Fig. 3a) due to the increased contribution of sea spray aerosol in winter months at the Zeppelin Observatory (Adachi et al., 2022; Zieger et al., 2010). This seasonality is due to increased wind speeds and prevalence of storms in winter that generate nascent sea spray from ocean surfaces and lift sea-salt-rich snow from ice-covered ocean (Adachi et al., 2022). The opposite behavior is observed by the contribution of fPBAPs to the coarse-mode cloud residuals (Fig. 3a), which was much higher in summer than in winter. The annual cycle of the cloud fPBAP population reflects that of the general fPBAP population at the Zeppelin Observatory (Pereira Freitas et al., 2023). These results seem to confirm the expectation that fPBAPs would act as efficient cloud nuclei (Ariya et al., 2009). At the beginning and end of summer, when the contribution of fPBAPs is higher and meteorological conditions are favorable, they potentially also contribute to the formation of MPCs by acting as INPs.

The d-excess within the CEs (Fig. 3b) shows high values for winter and low values for the remainder of the year. This implies that the moisture in winter air masses during cloudy periods was mainly sourced from long-range transport (Kopec et al., 2016). This agrees well with reports on the influence of lower latitudes on the Arctic aerosol population in winter (Sharma et al., 2006). The lower d-excess for the remainder of the year implies that moisture was more regionally sourced (Kopec et al., 2016; Delattre et al., 2015; Froehlich et al., 2002). The d-excess observations combined with back trajectory analyses link lower values to transport from terrestrial sources (Fig. S6). These results point to a

Table 1. Summary of detected fluorescent primary biological aerosol particles (fPBAPs) inside low-level Arctic clouds. Summer includes the months from June to September, while winter refers to October through May.

	fPBAPs measured (no.)	Number of cloud events (no.)	Total hours of sampled clouds (h)	Clouds containing fPBAPs (%)	fPBAP conc. (mean, $10^{-3}\,L^{-1}$)	fPBAP conc. (median, $10^{-3}\,L^{-1}$)	fPBAP contr. to coarse-mode cloud residuals (mean, %)	fPBAP contr. to coarse-mode cloud residuals (median, %)
Summer	476	156	612	67	8.1	4.8	0.032	0.012
Winter	51	53	200	45	4.3	0	0.005	0
$\frac{\text{Summer}}{\text{Winter}}$	9	2.9	3.1	1.47	-	–	–	–

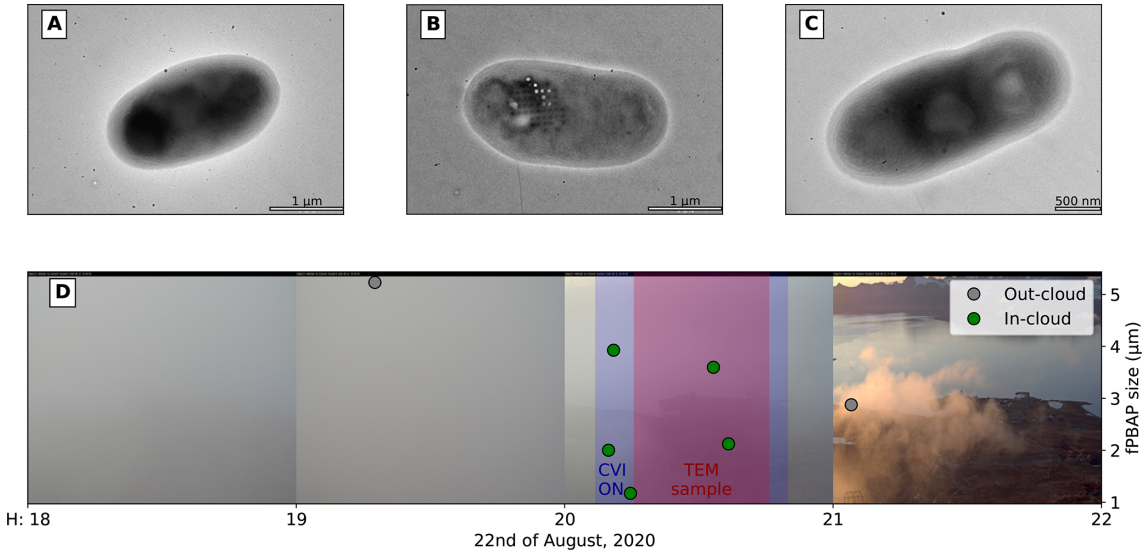

Figure 2. Example of primary biological aerosol particles (PBAPs) within cloud residuals as identified via transmission electron microscopy (TEM) and multiparameter bioaerosol spectrometer (MBS) analysis. Panels **(a)**–**(c)** show identified PBAPs on the TEM sample taken on 22 August 2020 (sampled downstream of the ground-based counterflow virtual impactor, CVI, inlet). Panel **(d)** shows webcam images (taken from Pedersen, 2013) of the cloud event and the periods of the CVI operation (blue area) and TEM sampling (pink area). In addition, the fluorescent PBAPs (fPBAPs) identified by the MBS are shown in the background as a function of their size (right axis). Out-cloud-measured fPBAPs (MBS sampling from a whole-air inlet) are shown for context. Dots on the particle shown in panel **(b)** are due to electron-beam-induced damage.

more pronounced terrestrial origin of cloud residual fPBAPs, corroborating previous work where fPBAPs detected at the Zeppelin Observatory were found to originate from regional and land-based sources (Pereira Freitas et al., 2023), including the polar semideserts that dominate the tundra of Svalbard (Welker et al., 1993; Wookey et al., 1995). Nonetheless, the ocean and sea ice can still be a significant source of fPBAPs and INPs, especially in winter (Creamean et al., 2019; Pereira Freitas et al., 2023). Moreover, the Svalbard region is notorious for being strongly affected by the Arctic amplification, prompting a dramatic change in annual sea ice coverage (Urbański and Litwicka, 2022). Thus, although our results point to terrestrial sources, fPBAPs sourced from regional marine and ice sources can still significantly contribute to the fPBAP population to a degree that is hard to estimate using our methods. DNA-based techniques, such as those applied by Šantl-Temkiv et al. (2019), could better constrain the sources of fPBAPs in the Arctic.

The ice-to-droplet ratio (Fig. 3c) shows that low-level clouds at Ny-Ålesund during the colder months (January–April and September–December) are mainly represented by ice clouds, whereas for July they are mainly represented by liquid droplets. For June and August, most clouds were MPCs, which reflects the findings of Mioche et al. (2015). Figure 3c shows that MPCs were mostly present at the beginning and end of summer, when there are suitable meteorological conditions and a higher contribution of fPBAPs to coarse-mode aerosol.

The ambient temperature at 475 m a.s.l. reached values as low as −25 °C in winter and values as high as 10 °C in summer (Fig. 3d). In the months that transition from summer to winter, the air temperature was on average around 0 °C. For May through September, the ambient temperature reached

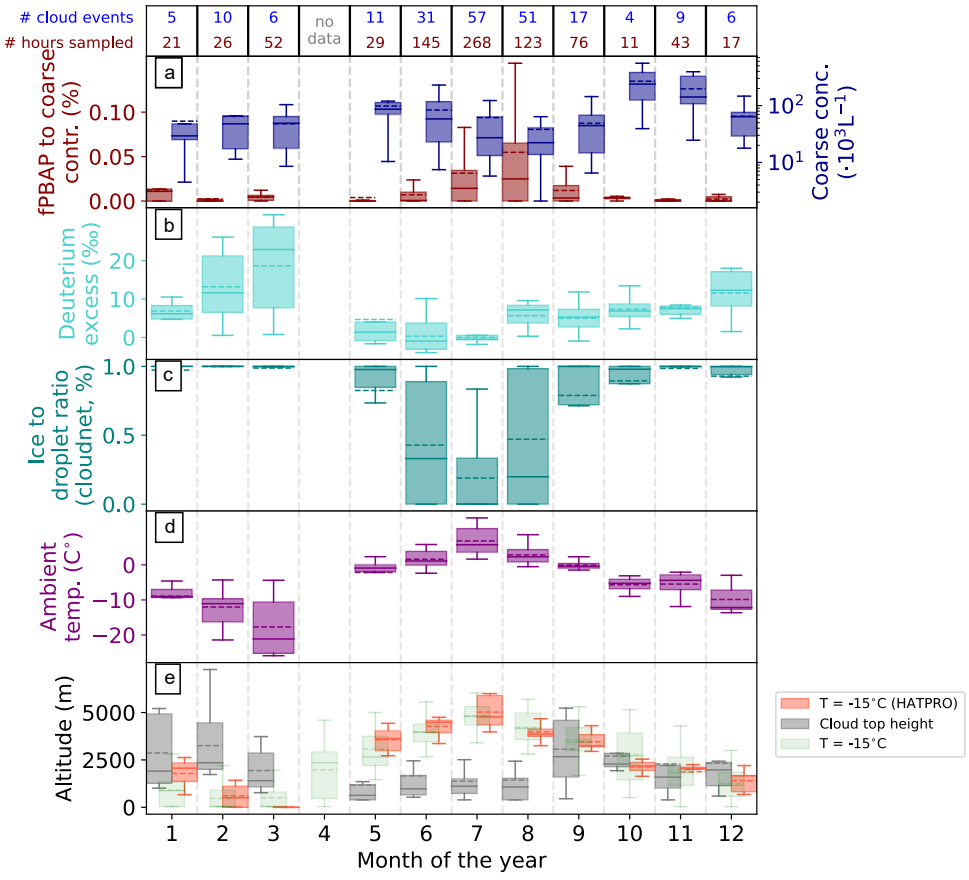

Figure 3. Annual cycles of all relevant bioaerosol, water vapor, cloud, and meteorological parameters during cloud events. Above panel **(a)** are the number of cloud events (CEs) and sampled hours per month of the year. For details on the availability of data, see Table S1. These values refer to all datasets except for temperature soundings in panel **(e)**. **(a)** Coarse aerosol (optical diameter > 0.8 µm) concentration as measured by the multiparameter bioaerosol spectrometer, along with the contribution of fluorescent primary biological aerosol particles (fPBAPs) to the coarse-mode cloud residuals (at the Zeppelin Observatory). **(b)** Water deuterium excess (d-excess, at the Zeppelin Observatory). **(c)** Ice-to-droplet ratio (measured above Ny-Ålesund at the height of the Zeppelin Observatory). **(d)** Ambient temperature (at the Zeppelin Observatory). **(e)** Altitude when air temperature is −15 °C) as measured by daily atmospheric soundings from 2019–2006 to 2020–2012 and per CE by the HATPRO measured above Ny-Ålesund at the height of the Zeppelin Observatory. Furthermore, the cloud top height of the lowest cloud is also shown.

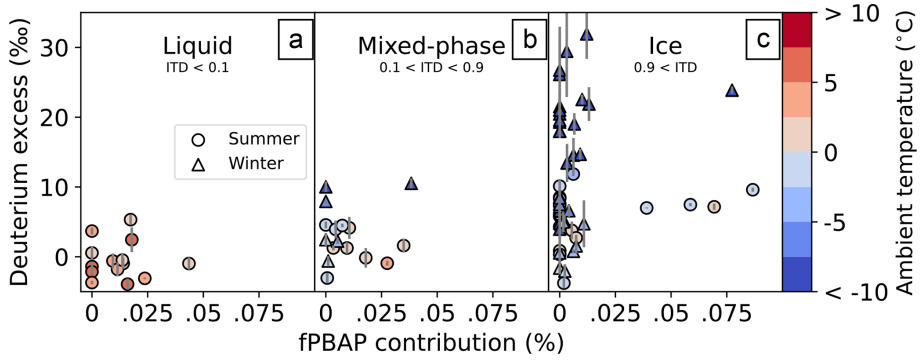

Figure 4. Deuterium excess (d-excess) vs. fluorescent primary biological aerosol particle (fPBAP) contribution to aerosol coarse-mode number concentration. Relationship shown for **(a)** liquid, **(b)** mixed-phase, and **(c)** ice cloud events as classified by the ice-to-droplet (ITD) ratio. Colors represent the mean ambient temperature at 475 m a.s.l. Triangles denote clouds in winter while circles show summer cloud events. Individual points are arithmetic mean values, and error bars represent the corresponding standard deviation of d-excess.

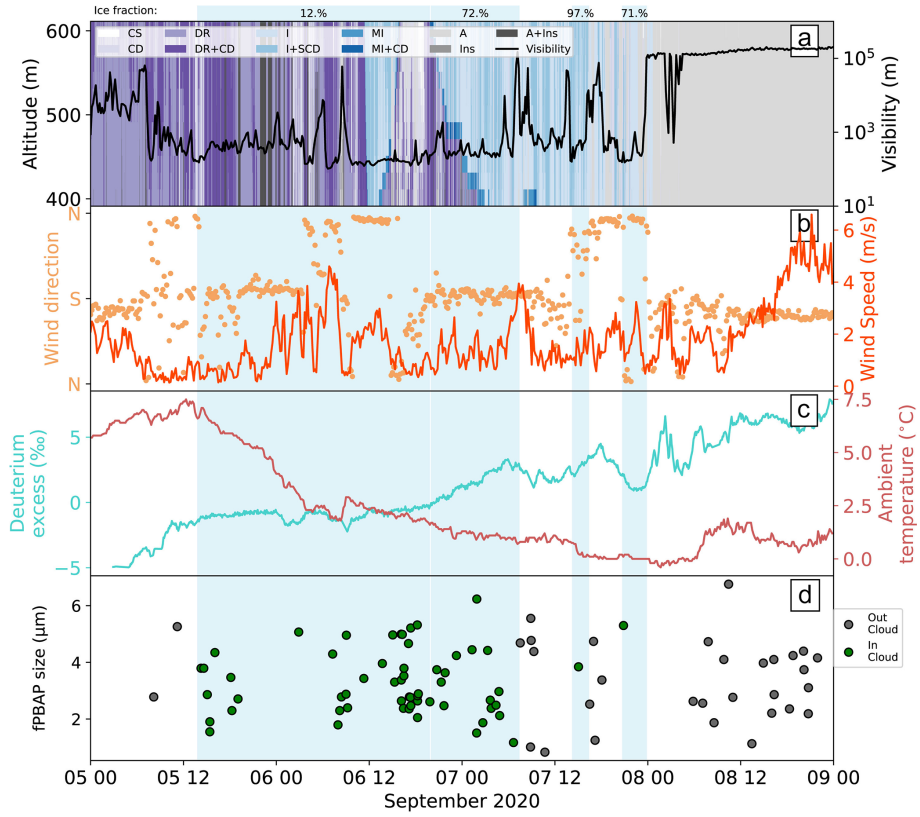

Figure 5. Example of a mixed-phase cloud event measured in September 2020. **(a)** Cloudnet classification (at the height of the Zeppelin Observatory) and visibility (directly measured at the Zeppelin Observatory). Light-blue boxes above and in the panels indicate periods where counterflow virtual impactor (CVI) inlet sampling occurred along with the ice fraction of each CVI cloud event calculated using the Cloudnet data. **(b)** Wind direction and speed at the Zeppelin Observatory. **(c)** Water vapor deuterium excess and ambient temperature. **(d)** Fluorescent primary biological aerosol particles (fPBAPs) measured and categorized by size. Out-cloud fPBAPs are shown for context.

−15 °C only at altitudes higher than 2500 m. This can be seen in Fig. 3e, derived by both daily radio soundings and continuous HATPRO vertical temperature profiling above the village of Ny-Ålesund. The cloud top height of low-level clouds was much higher in the beginning of the year, reaching its minima in summer, where it stayed below 2500 m. Thus, the temperatures across the air columns in summer point to the requirement of high-temperature INPs for ice formation to occur.

These results are an early but clear indication of the contribution of fPBAPs to MPCs in the Arctic. For a more comprehensive understanding of the PBAPs' role in Arctic MPC formation, a combination of single-particle cloud probes and CVI would allow for distinction between individual ice and droplet particles.

3.4 Relationship between cloud phase, bioaerosol contribution, and isotope ratio

Figure 4 shows the d-excess rate vs. the fPBAP contribution to the coarse-mode cloud residual concentration for three cloud regimes grouped by winter and summer seasons. In Fig. 4a, liquid clouds appear only in summer and present high ambient air temperatures, as expected (Ebell et al., 2020). Low d-excess values link the water vapor to air masses of predominantly regional origin. These clouds had a fPBAP contribution of 0.01 %. MPCs are present mainly in summer and at mild temperatures (from −5 to 5 °C, Fig. 4b). Most of them seem to originate from regional air masses, as indicated by the low d-excess values. For MPCs at mild temperatures (from −5 to 5 °C), fPBAP contribution was 0.01 % or higher. Ice clouds were predominantly seen in winter (Fig. 4c). Those observed in summer were present at mild temperatures (−5 to 5 °C) and typically had a low d-excess value. A few ice clouds were highly enriched in fPBAPs (values above 0.025 %) with d-excess rates at around 10 ‰, indicating a mix between regional and transported sources.

These results show that summer clouds containing ice were present at mild temperatures and often contained fPBAPs (> 0.01 %), indicating the role of fPBAPs in ice formation. For all cloud-phase regimes, fPBAPs were mostly present at lower d-excess values. Regional aerosol sources are important for cloud formation and evolution in the Arctic (Gierens et al., 2020), and this seems to be reflected here.

3.5 Mixed-phase cloud event analysis

From 5 to the 8 of September 2020, the Zeppelin Observatory was continuously in cloud. Initially, the Cloudnet classification was mostly consistent with a liquid cloud, with an increase in ice contribution towards the second half. For the first CE, the ice fraction was 12 %. The cloud glaciated and transitioned to containing almost only ice crystals before dissipating or migrating (up to 97 % of ice; Fig. 5a). Visibility remained below 1000 m for most of the cloud. Wind speeds hovered around 2 m s^{-1} with a persistent southerly direction except for a few hours when it switched to northerly winds (Fig. 5b). These long-lasting MPCs are common for the Arctic (Morrison et al., 2012).

The d-excess from the cloud water vapor started at −5 ‰ and ended at around 0 ‰. This small change and the overall low values signal that the air mass was of regional origin (Kopec et al., 2016; Fig. 5c). The water vapor and aerosol source might not be identical, whereas the latter could be a mix between regional emissions (e.g., Pereira Freitas et al., 2023) and emissions transported over a long range (e.g., Behrenfeldt et al., 2008; Geng et al., 2010; Creamean et al., 2022). Coarse-mode aerosol is comprised of larger particles that are effectively removed by dry and wet deposition (Stopelli et al., 2015) but are occasionally transported to the Arctic from lower latitudes (Behrenfeldt et al., 2008). The precipitation process along the path of transported air masses will lead to the depletion of d-excess values and the wet removal of coarse-mode aerosol. However, we cannot use the d-excess to decisively link the cloud aerosol population to regional sources.

The cloud temperature at 475 m a.s.l. was 7.5 °C at the start of the cloud and continuously dropped to 0 °C towards the end of the cloud as it glaciated. For this day, the air temperature reached values of −15 °C only at approximately 4000 m a.s.l. and the height of the cloud top was approximately 1600 m (temperature at cloud top height: ≈ −8 °C; Fig. S7). Thus, a likely explanation for the presence of ice within this cloud is ice nucleation started by high-temperature INPs (Fan et al., 2017), of which fPBAPs are part of Tobo et al. (2013), or secondary ice formation due to, e.g., ice crystals being deposited by clouds higher up in the atmosphere (Lohmann et al., 2016).

As the cloud developed, fPBAPs were clearly detected by the MBS within the cloud residuals. A total of 58 fPBAPs were found within the cloud (over four CEs), accounting for 2 in every 10^4 coarse-mode particles. The presence of fPBAPs could be one of the explanations for cloud glaciation at temperatures at which the presence of high-temperature INPs would be required. However, further studies assessing the role of other glaciation mechanisms (such as precipitation from clouds higher in the column) are required to fully establish the impact of fPBAPs (and INPs) on low-level Arctic clouds.

4 Conclusions

Within this work, we showed that fluorescent primary biological aerosol particles (fPBAPs) are found within cloud residuals and possibly contributed to the formation of low-level Arctic clouds. This was achieved, for the first time, by direct observations using a ground-based counterflow virtual impactor inlet combined with online and offline particle sampling techniques. This approach avoided indirect proof of the relevance of fPBAPs for cloud properties, for example, when using correlations of INPs with fPBAP concentrations as done previously (Pereira Freitas et al., 2023). fPBAPs exhibited higher concentrations (10^{-3}–10^{-2} L^{-1}) and contributions (0.1 to 1 in 10^3 particles) to the coarse-mode cloud residuals in summer compared to winter (10^{-4}–10^{-3} L^{-1}, and 1 in 10^4–10^5 particles, respectively). In summer, water vapor isotope data linked clouds to regional sources. Thus, fPBAPs most likely originated from the biosphere around Svalbard. The presence of fPBAPs was associated with the prevalence of mixed-phase clouds at the beginning and end of summer. Here, we present experimental and direct evidence that fPBAPs contribute to ice formation in Arctic low-level clouds. However, cloud formation is a complex phenomenon involving meteorology as well as interlinked cloud and aerosol microphysical and chemical processes. Thus, the degree to which fPBAPs influence cloud glaciation in general would require further investigation through both experimental (e.g., by quantitative assessment of the cloud phase using single-particle cloud probes) and modeling approaches. Future work should also include filter sampling for genetic analysis to identify the biological material and origin, in addition to parallel sampling of bioaerosols within cloud residuals and interstitial aerosol to assess whether certain microorganisms are more likely to act as cloud condensation nuclei.

Data availability. The data are available at the Bolin Centre for Climate Research database (https://doi.org/10.17043/zeppelin-freitas-2023-bioclouds-1, Pereira Freitas et al., 2024).

Supplement. The supplement related to this article is available online at: https://doi.org/10.5194/acp-24-5479-2024-supplement.

Author contributions. GPF, RK, and PZ performed MBS and CVI measurements. KA performed TEM measurements. GPF analyzed MBS, CVI, and auxiliary data and wrote the manuscript with contributions from all co-authors. BK, AH, and JMW performed water isotope measurements and performed analysis. DHR performed back trajectory analysis. KEY provided valuable insights to the discussion and writing of the manuscript. PZ conceived the study. All authors read and commented on the final version of the manuscript.

Competing interests. At least one of the (co-)authors is a member of the editorial board of *Atmospheric Chemistry and Physics*. The peer-review process was guided by an independent editor, and the authors also have no other competing interests to declare.

Disclaimer. Publisher's note: Copernicus Publications remains neutral with regard to jurisdictional claims made in the text, published maps, institutional affiliations, or any other geographical representation in this paper. While Copernicus Publications makes every effort to include appropriate place names, the final responsibility lies with the authors.

Acknowledgements. The authors would like to acknowledge the Norwegian Polar Institute for their long-term support at the Zeppelin Observatory. We thank Tabea Hennig, Zahra Hamzavi, Birgitta Noone, and Kai Rosman for their excellent technical support. The authors thank Valtteri Hyoky for on-site support and data processing for the isotopic measurements at the Zeppelin Observatory. The authors are grateful for the support and collaboration with the University of Hertfordshire related to the development and support of the MBS instrument (Paul Kaye and Warren Stanley).

Financial support. This research was supported by the Swedish Research Council (grant no. 2018-05045), the Knut och Alice Wallenbergs Stiftelse (ACAS project, grant no. 2016.0024), and the Swedish Environmental Agency (Naturvårdsverket). This project has received funding from the European Union's Horizon 2020 research and innovation programme under grant agreement no. 821205 (FORCeS). This project has received funding from the European Union's Horizon 2020 research and innovation programme under grant no. 101003826 via project CRiceS (Climate Relevant interactions and feedbacks: the key role of sea ice and Snow in the polar and global climate system). We thank the Environmental Research and Technology Development Fund (grant no. JPMEERF20232001) of the Environmental Restoration and Conservation Agency of Japan and the Arctic Challenge for Sustainability II (ArCS II) (grant no. JPMXD1420318865). Water isotopic measurements at the Zeppelin were supported by the Academy of Finland award to Jeffrey M. Welker and Alun Hubbard. Alun Hubbard gratefully acknowledges an Arctic Five Chair ("Rainmaker"), funding from the Research Council of Norway through its Centres of Excellence scheme (projects 223259 and 332635), and a research fellowship at the University of Oulu funded by Arctic Interactions, Academy of Finland PROFI4 (grant no. 318930) and the FARIA network.

The article processing charges for this open-access publication were covered by Stockholm University.

Review statement. This paper was edited by James Allan and reviewed by two anonymous referees.

References

Adachi, K., Oshima, N., Gong, Z., de Sá, S., Bateman, A. P., Martin, S. T., de Brito, J. F., Artaxo, P., Cirino, G. G., Sedlacek III, A. J., and Buseck, P. R.: Mixing states of Amazon basin aerosol particles transported over long distances using transmission electron microscopy, Atmos. Chem. Phys., 20, 11923–11939, https://doi.org/10.5194/acp-20-11923-2020, 2020.

Adachi, K., Tobo, Y., Koike, M., Freitas, G., Zieger, P., and Krejci, R.: Composition and mixing state of Arctic aerosol and cloud residual particles from long-term single-particle observations at Zeppelin Observatory, Svalbard, Atmos. Chem. Phys., 22, 14421–14439, https://doi.org/10.5194/acp-22-14421-2022, 2022.

Akers, P. D., Kopec, B. G., Mattingly, K. S., Klein, E. S., Causey, D., and Welker, J. M.: Baffin Bay sea ice extent and synoptic moisture transport drive water vapor isotope (δ18O, δ2H, and deuterium excess) variability in coastal northwest Greenland, Atmos. Chem. Phys., 20, 13929–13955, https://doi.org/10.5194/acp-20-13929-2020, 2020.

Ariya, P. A., Sun, J., Eltouny, N. A., Hudson, E. D., Hayes, C. T., and Kos, G.: Physical and chemical characterization of bioaerosols – Implications for nucleation processes, Int. Rev. Phys. Chem., 28, 1–32, https://doi.org/10.1080/01442350802597438, 2009.

Bailey, H., Hubbard, A., Klein, E. S., Mustonen, K. R., Akers, P. D., Marttila, H., and Welker, J. M.: Arctic sea-ice loss fuels extreme European snowfall, Nat. Geosci., 14, 283–288, https://doi.org/10.1038/s41561-021-00719-y, 2021.

Bauer, H., Kasper-Giebl, A., Löflund, M., Giebl, H., Hitzenberger, R., Zibuschka, F., and Puxbaum, H.: The contribution of bacteria and fungal spores to the organic carbon content of cloud water, precipitation and aerosols, Atmos. Res., 64, 109–119, https://doi.org/10.1016/S0169-8095(02)00084-4, 2002.

Bauer, H., Giebl, H., Hitzenberger, R., Kasper-Giebl, A., Reischl, G., Zibuschka, F., and Puxbaum, H.: Airborne bacteria as cloud condensation nuclei, J. Geophys. Res.-Atmos., 108, 4658, https://doi.org/10.1029/2003jd003545, 2003.

Behrenfeldt, U., Krejci, R., Ström, J., and Stohl, A.: Chemical properties of Arctic aerosol particles collected at the Zeppelin station during the aerosol transition period in May and June of 2004, Tellus B, 60, 405–415, https://doi.org/10.1111/j.1600-0889.2008.00349.x, 2008.

Bonne, J., Steen-Larsen, H. C., Risi, C., Werner, M., Sodemann, H., Lacour, J., Fettweis, X., Cesana, G., Delmotte, M., Cattani, O., Vallelonga, P., Kjær, H. A., Clerbaux, C., Sveinbjörnsdóttir, Ó. E., and Masson-Delmotte, V.: The summer 2012 Greenland heat wave: In situ and remote sensing observations of water vapor isotopic composition during an atmospheric river event, J. Geophys. Res.-Atmos., 120, 2970–2989, https://doi.org/10.1002/2014JD022602, 2015.

Bonne, J.-L., Behrens, M., Meyer, H., Kipfstuhl, S., Rabe, B., Schönicke, L., Steen-Larsen, H. C., and Werner, M.: Resolving the controls of water vapour isotopes in the Atlantic sector, Nat. Commun., 10, 1632, https://doi.org/10.1038/s41467-019-09242-6, 2019.

Carlsen, T. and David, R. O.: Spaceborne Evidence That Ice-Nucleating Particles Influence High-Latitude Cloud Phase, Geophys. Res. Lett., 49, 1–11, https://doi.org/10.1029/2022GL098041, 2022.

Chellini, G., Gierens, R., and Kneifel, S.: Ice Aggregation in Low-Level Mixed-Phase Clouds at a High Arctic Site: Enhanced by Dendritic Growth and Absent Close to the Melting Level, J. Geophys. Res.-Atmos., 127, 1–23, https://doi.org/10.1029/2022JD036860, 2022.

Copernicus Climate Change Service: (C3S) Climate Data Store (CDS): Sea ice concentration daily gridded data from 1979 to present derived from satellite observations, https://doi.org/10.24381/cds.3cd8b812, 2020.

Crawford, I., Gallagher, M. W., Bower, K. N., Choularton, T. W., Flynn, M. J., Ruske, S., Listowski, C., Brough, N., Lachlan-Cope, T., Fleming, Z. L., Foot, V. E., and Stanley, W. R.: Real-time detection of airborne fluorescent bioparticles in Antarctica, Atmos. Chem. Phys., 17, 14291–14307, https://doi.org/10.5194/acp-17-14291-2017, 2017.

Crawford, I., Topping, D., Gallagher, M., Forde, E., Lloyd, J. R., Foot, V., Stopford, C., and Kaye, P.: Detection of airborne biological particles in indoor air using a real-time advanced morphological parameter uv-lif spectrometer and gradient boosting ensemble decision tree classifiers, Atmosphere, 11, 1039, https://doi.org/10.3390/atmos11101039, 2020.

Creamean, J. M., Kirpes, R. M., Pratt, K. A., Spada, N. J., Maahn, M., de Boer, G., Schnell, R. C., and China, S.: Marine and terrestrial influences on ice nucleating particles during continuous springtime measurements in an Arctic oilfield location, Atmos. Chem. Phys., 18, 18023–18042, https://doi.org/10.5194/acp-18-18023-2018, 2018.

Creamean, J. M., Cross, J. N., Pickart, R., McRaven, L., Lin, P., Pacini, A., Hanlon, R., Schmale, D. G., Ceniceros, J., Aydell, T., Colombi, N., Bolger, E., and DeMott, P. J.: Ice Nucleating Particles Carried From Below a Phytoplankton Bloom to the Arctic Atmosphere, Geophys. Res. Lett., 46, 8572–8581, https://doi.org/10.1029/2019GL083039, 2019.

Creamean, J. M., Barry, K., Hill, T. C., Hume, C., DeMott, P. J., Shupe, M. D., Dahlke, S., Willmes, S., Schmale, J., Beck, I., Hoppe, C. J., Fong, A., Chamberlain, E., Bowman, J., Scharien, R., and Persson, O.: Annual cycle observations of aerosols capable of ice formation in central Arctic clouds, Nat. Commun., 13, 1–12, https://doi.org/10.1038/s41467-022-31182-x, 2022.

Cross, M.: PySPLIT: a Package for the Generation, Analysis, and Visualization of HYSPLIT Air Parcel Trajectories, 133–137, https://doi.org/10.25080/Majora-7b98e3ed-014, 2015.

Curry, J. A. and Ebert, E. E.: Annual Cycle of Radiation Fluxes over the Arctic Ocean: Sensitivity to Cloud Optical Properties, J. Clim., 5, 1267–1280, https://doi.org/10.1175/1520-0442(1992)005<1267:ACORFO>2.0.CO;2, 1992.

Dansgaard, W.: Stable isotopes in precipitation, Tellus A, 16, 436–468, https://doi.org/10.3402/tellusa.v16i4.8993, 2012.

Delattre, H., Vallet-Coulomb, C., and Sonzogni, C.: Deuterium excess in the atmospheric water vapour of a Mediterranean coastal wetland: regional vs. local signatures, Atmos. Chem. Phys., 15, 10167–10181, https://doi.org/10.5194/acp-15-10167-2015, 2015.

Després, V. R., Alex Huffman, J., Burrows, S. M., Hoose, C., Safatov, A. S., Buryak, G., Fröhlich-Nowoisky, J., Elbert, W., Andreae, M. O., Pöschl, U., and Jaenicke, R.: Primary biological aerosol particles in the atmosphere: A review, Tellus B, 64, 15598, https://doi.org/10.3402/tellusb.v64i0.15598, 2012.

Draxler, R. R., Spring, S., Maryland, U. S. A., and Hess, G. D.: An Overview of the HYSPLIT_4 Modelling System for Trajectories, Dispersion, and Deposition, Austr. Meteorol. Mag., 47, 295–308, 1998.

Ebell, K., Nomokonova, T., Maturilli, M., and Ritter, C.: Radiative effect of clouds at ny-Ålesund, svalbard, as inferred from ground-based remote sensing observations, J. Appl. Meteorol. Climatol., 59, 3–22, https://doi.org/10.1175/JAMC-D-19-0080.1, 2020.

Fan, J., Leung, L. R., Rosenfeld, D., and DeMott, P. J.: Effects of cloud condensation nuclei and ice nucleating particles on precipitation processes and supercooled liquid in mixed-phase orographic clouds, Atmos. Chem. Phys., 17, 1017–1035, https://doi.org/10.5194/acp-17-1017-2017, 2017.

Freitas, G. P., Stolle, C., Kaye, P. H., Stanley, W., Herlemann, D. P., Salter, M. E., and Zieger, P.: Emission of primary bioaerosol particles from Baltic seawater, Environ. Sci.-Atmos., 2022, 1170–1182, https://doi.org/10.1039/d2ea00047d, 2022.

Froehlich, K., Gibson, J. J., and Aggarwal, P. K.: Deuterium excess in precipitation and its climatological significance, International Atomic Energy Agency, Vienna (Austria), United Nations Educational, Scientific and Cultural Organization, Paris (France), Japan Science and Technology Corporation (Japan), 541 pp., October 2002, 54–66, International conference on study of environmental change using isotope techniques, Vienna (Austria), 23–27 April 2001, IAEA-CN–80/104, ISSN 1563-0153, 2002.

Fröhlich-Nowoisky, J., Kampf, C. J., Weber, B., Huffman, J. A., Pöhlker, C., Andreae, M. O., Lang-Yona, N., Burrows, S. M., Gunthe, S. S., Elbert, W., Su, H., Hoor, P., Thines, E., Hoffmann, T., Després, V. R., and Pöschl, U.: Bioaerosols in the Earth system: Climate, health, and ecosystem interactions, Atmos. Res., 182, 346–376, https://doi.org/10.1016/j.atmosres.2016.07.018, 2016.

Geng, H., Ryu, J., Jung, H.-J., Chung, H., Ahn, K.-H., and Ro, C.-U.: Single-Particle Characterization of Summertime Arctic Aerosols Collected at Ny-Ålesund, Svalbard, Environ. Sci. Technol., 44, 2348–2353, https://doi.org/10.1021/es903268j, 2010.

Gierens, R., Kneifel, S., Shupe, M. D., Ebell, K., Maturilli, M., and Löhnert, U.: Low-level mixed-phase clouds in a complex Arctic environment, Atmos. Chem. Phys., 20, 3459–3481, https://doi.org/10.5194/acp-20-3459-2020, 2020.

Gramlich, Y., Siegel, K., Haslett, S. L., Freitas, G., Krejci, R., Zieger, P., and Mohr, C.: Revealing the chemical characteristics of Arctic low-level cloud residuals – in situ observations from a mountain site, Atmos. Chem. Phys., 23, 6813–6834, https://doi.org/10.5194/acp-23-6813-2023, 2023.

Hartmann, M., Adachi, K., Eppers, O., Haas, C., Herber, A., Holzinger, R., Hünerbein, A., Jäkel, E., Jentzsch, C., van Pinxteren, M., Wex, H., Willmes, S., and Stratmann, F.: Wintertime Airborne Measurements of Ice Nucleating Particles in the High Arctic: A Hint to a Marine, Biogenic Source for Ice Nucleating Particles, Geophys. Res. Lett., 47, e2020GL087770, https://doi.org/10.1029/2020GL087770, 2020.

Huffman, J. A., Perring, A. E., Savage, N. J., Clot, B., Crouzy, B., Tummon, F., Shoshanim, O., Damit, B., Schneider, J., Sivaprakasam, V., Zawadowicz, M. A., Crawford, I., Gallagher, M., Topping, D., Doughty, D. C., Hill, S. C.,

and Pan, Y.: Real-time sensing of bioaerosols: Review and current perspectives, Aerosol Sci. Technol., 54, 465–495, https://doi.org/10.1080/02786826.2019.1664724, 2020.

Illingworth, A. J., Hogan, R. J., O'Connor, E. J., Bouniol, D., Brooks, M. E., Delanoë, J., Donovan, D. P., Eastment, J. D., Gaussiat, N., Goddard, J. W., Haeffelin, M., Klein Baltinik, H., Krasnov, O. A., Pelon, J., Piriou, J. M., Protat, A., Russchenberg, H. W., Seifert, A., Tompkins, A. M., van Zadelhoff, G. J., Vinit, F., Willen, U., Wilson, D. R., and Wrench, C. L.: Cloudnet: Continuous evaluation of cloud profiles in seven operational models using ground-based observations, Bull. Am. Meteorol. Soc., 88, 883–898, https://doi.org/10.1175/BAMS-88-6-883, 2007.

Joly, M., Attard, E., Sancelme, M., Deguillaume, L., Guilbaud, C., Morris, C. E., Amato, P., and Delort, A. M.: Ice nucleation activity of bacteria isolated from cloud water, Atmos. Environ., 70, 392–400, https://doi.org/10.1016/j.atmosenv.2013.01.027, 2013.

Kanji, Z. A., Ladino, L. A., Wex, H., Boose, Y., Burkert-Kohn, M., Cziczo, D. J., and Krämer, M.: Overview of Ice Nucleating Particles, Meteorol. Monogr., 58, 1.1–1.33, https://doi.org/10.1175/amsmonographs-d-16-0006.1, 2017.

Karlsson, L., Krejci, R., Koike, M., Ebell, K., and Zieger, P.: A long-term study of cloud residuals from low-level Arctic clouds, Atmos. Chem. Phys., 21, 8933–8959, https://doi.org/10.5194/acp-21-8933-2021, 2021.

Karlsson, L., Baccarini, A., Duplessis, P., Baumgardner, D., Brooks, I. M., Chang, R. Y., Dada, L., Dällenbach, K. R., Heikkinen, L., Krejci, R., Leaitch, W. R., Leck, C., Partridge, D. G., Salter, M. E., Wernli, H., Wheeler, M. J., Schmale, J., and Zieger, P.: Physical and Chemical Properties of Cloud Droplet Residuals and Aerosol Particles During the Arctic Ocean 2018 Expedition, J. Geophys. Res.-Atmos., 127, 1–20, https://doi.org/10.1029/2021JD036383, 2022.

Kay, J. E., L'Ecuyer, T., Chepfer, H., Loeb, N., Morrison, A., and Cesana, G.: Recent Advances in Arctic Cloud and Climate Research, Curr. Clim. Change Rep., 2, 159–169, https://doi.org/10.1007/s40641-016-0051-9, 2016.

Khaled, A., Zhang, M., Amato, P., Delort, A.-M., and Ervens, B.: Biodegradation by bacteria in clouds: an underestimated sink for some organics in the atmospheric multiphase system, Atmos. Chem. Phys., 21, 3123–3141, https://doi.org/10.5194/acp-21-3123-2021, 2021.

Kopec, B. G., Feng, X., Michel, F. A., and Posmentier, E. S.: Influence of sea ice on Arctic precipitation, P. Natl. Acad. Sci. USA, 113, 46–51, https://doi.org/10.1073/pnas.1504633113, 2016.

Korolev, A. V., Isaac, G. A., Cober, S. G., Strapp, J. W., and Hallett, J.: Microphysical characterization of mixed-phase clouds, Q. J. Roy. Meteorol. Soc., 129, 39–65, https://doi.org/10.1256/qj.01.204, 2003.

Lensky, I. M. and Rosenfeld, D.: Satellite-based insights into precipitation formation processes in continental and maritime convective clouds at nighttime, J. Appl. Meteorol., 42, 1227–1233, https://doi.org/10.1175/1520-0450(2003)042<1227:SIIPFP>2.0.CO;2, 2003.

Lohmann, U., Lüönd, F., and Mahrt, F.: An Introduction to Clouds: From the Microscale to Climate, Cambridge University Press, Cambridge, https://doi.org/10.1017/CBO9781139087513, 2016.

Maturilli, M.: High resolution radiosonde measurements from station Ny-Ålesund (2017-04 et seq), PANGAEA, https://doi.org/10.1594/PANGAEA.914973, 2020.

Maturilli, M. and Ebell, K.: Twenty-five years of cloud base height measurements by ceilometer in Ny-Ålesund, Svalbard, Earth Syst. Sci. Data, 10, 1451–1456, https://doi.org/10.5194/essd-10-1451-2018, 2018.

Matus, A. V. and L'Ecuyer, T. S.: The role of cloud phase in Earth's radiation budget, J. Geophys. Res., 122, 2559–2578, https://doi.org/10.1002/2016JD025951, 2017.

Meinander, O., Dagsson-Waldhauserova, P., Amosov, P., Aseyeva, E., Atkins, C., Baklanov, A., Baldo, C., Barr, S. L., Barzycka, B., Benning, L. G., Cvetkovic, B., Enchilik, P., Frolov, D., Gassó, S., Kandler, K., Kasimov, N., Kavan, J., King, J., Koroleva, T., Krupskaya, V., Kulmala, M., Kusiak, M., Lappalainen, H. K., Laska, M., Lasne, J., Lewandowski, M., Luks, B., McQuaid, J. B., Moroni, B., Murray, B., Möhler, O., Nawrot, A., Nickovic, S., O'Neill, N. T., Pejanovic, G., Popovicheva, O., Ranjbar, K., Romanias, M., Samonova, O., Sanchez-Marroquin, A., Schepanski, K., Semenkov, I., Sharapova, A., Shevnina, E., Shi, Z., Sofiev, M., Thevenet, F., Thorsteinsson, T., Timofeev, M., Umo, N. S., Uppstu, A., Urupina, D., Varga, G., Werner, T., Arnalds, O., and Vukovic Vimic, A.: Newly identified climatically and environmentally significant high-latitude dust sources, Atmos. Chem. Phys., 22, 11889–11930, https://doi.org/10.5194/acp-22-11889-2022, 2022.

Merlivat, L. and Jouzel, J.: Global climatic interpretation of the deuterium-oxygen 18 relationship for precipitation, J. Geophys. Res.-Ocean., 84, 5029–5033, https://doi.org/10.1029/JC084iC08p05029, 1979.

Mioche, G., Jourdan, O., Ceccaldi, M., and Delanoë, J.: Variability of mixed-phase clouds in the Arctic with a focus on the Svalbard region: a study based on spaceborne active remote sensing, Atmos. Chem. Phys., 15, 2445–2461, https://doi.org/10.5194/acp-15-2445-2015, 2015.

Morrison, H., De Boer, G., Feingold, G., Harrington, J., Shupe, M. D., and Sulia, K.: Resilience of persistent Arctic mixed-phase clouds, Nat. Geosci., 5, 11–17, https://doi.org/10.1038/ngeo1332, 2012.

Nomokonova, T., Ebell, K., Löhnert, U., Maturilli, M., Ritter, C., and O'Connor, E.: Statistics on clouds and their relation to thermodynamic conditions at Ny-Ålesund using ground-based sensor synergy, Atmos. Chem. Phys., 19, 4105–4126, https://doi.org/10.5194/acp-19-4105-2019, 2019.

Nomokonova, T., Ebell, K., Löhnert, U., Maturilli, M., and Ritter, C.: The influence of water vapor anomalies on clouds and their radiative effect at Ny-Ålesund, Atmos. Chem. Phys., 20, 5157–5173, https://doi.org/10.5194/acp-20-5157-2020, 2020.

Noone, D., Galewsky, J., Sharp, Z. D., Worden, J., Barnes, J., Baer, D., Bailey, A., Brown, D. P., Christensen, L., Crosson, E., Dong, F., Hurley, J. V., Johnson, L. R., Strong, M., Toohey, D., Van Pelt, A., and Wright, J. S.: Properties of air mass mixing and humidity in the subtropics from measurements of the D/H isotope ratio of water vapor at the Mauna Loa Observatory, J. Geophys. Res.-Atmos., 116, D22113, https://doi.org/10.1029/2011JD015773, 2011.

Noone, K. J., Ogren, J. A., Heintzenberg, J., Charlson, R. J., and Covert, D. S.: Design and calibration of a counterflow virtual impactor for sampling of atmospheric fog and cloud droplets, Aerosol Sci. Technol., 8, 235–244, https://doi.org/10.1080/02786828808959186, 1988.

Pasquier, J. T., David, R. O., Freitas, G., Gierens, R., Gramlich, Y., Haslett, S., Li, G., Schäfer, B., Siegel, K., Wieder, J., Adachi, K., Belosi, F., Carlsen, T., Decesari, S., Ebell, K., Gilardoni, S., Gysel-Beer, M., Henneberger, J., Inoue, J., Kanji, Z. A., Koike, M., Kondo, Y., Krejci, R., Lohmann, U., Maturilli, M., Mazzolla, M., Modini, R., Mohr, C., Motos, G., Nenes, A., Nicosia, A., Ohata, S., Paglione, M., Park, S., Pileci, R. E., Ramelli, F., Rinaldi, M., Ritter, C., Sato, K., Storelvmo, T., Tobo, Y., Traversi, R., Viola, A., and Zieger, P.: The Ny-Ålesund Aerosol Cloud Experiment (NASCENT) Overview and First Results, Bull. Am. Meteorol. Soc., 103, E2533–E2558, https://doi.org/10.1175/BAMS-D-21-0034.1, 2022.

Pedersen, C.: Zeppelin Webcamera Time Series, Norwegian Polar Data Centre [data set], https://doi.org/10.21334/npolar.2013.9fd6dae0, 2013.

Pereira Freitas, G., Adachi, K., Conen, F., Heslin-Rees, D., Krejci, R., Tobo, Y., Yttri, K. E., and Zieger, P.: Regionally sourced bioaerosols drive high-temperature ice nucleating particles in the Arctic, Nat. Commun., 14, 5997, https://doi.org/10.1038/s41467-023-41696-7, 2023.

Pereira Freitas, G., Krejci, R., Heslin-Rees, D., Kopec, B., Hubbard, A., Welker, J. M., and Zieger, P.: Fluorescent primary biological aerosol particle concentrations in low-level Arctic cloud residuals in Svalbard 2019–2021, Dataset version 1, Bolin Centre Database [data set], https://doi.org/10.17043/zeppelin-freitas-2023-bioclouds-1, 2024.

Pöhlker, C., Huffman, J. A., and Pöschl, U.: Autofluorescence of atmospheric bioaerosols – fluorescent biomolecules and potential interferences, Atmos. Meas. Tech., 5, 37–71, https://doi.org/10.5194/amt-5-37-2012, 2012.

Porter, G. C., Adams, M. P., Brooks, I. M., Ickes, L., Karlsson, L., Leck, C., Salter, M. E., Schmale, J., Siegel, K., Sikora, S. N., Tarn, M. D., Vüllers, J., Wernli, H., Zieger, P., Zinke, J., and Murray, B. J.: Highly Active Ice-Nucleating Particles at the Summer North Pole, J. Geophys. Res.-Atmos., 127, 1–18, https://doi.org/10.1029/2021JD036059, 2022.

Prenni, A. J., Harrington, J. Y., Tjernström, M., DeMott, P. J., Avramov, A., Long, C. N., Kreidenweis, S. M., Olsson, P. Q., and Verlinde, J.: Can ice-nucleating aerosols affect arctic seasonal climate?, Bull. Am. Meteorol. Soc., 88, 541–550, 2007.

Pummer, B. G., Budke, C., Augustin-Bauditz, S., Niedermeier, D., Felgitsch, L., Kampf, C. J., Huber, R. G., Liedl, K. R., Loerting, T., Moschen, T., Schauperl, M., Tollinger, M., Morris, C. E., Wex, H., Grothe, H., Pöschl, U., Koop, T., and Fröhlich-Nowoisky, J.: Ice nucleation by water-soluble macromolecules, Atmos. Chem. Phys., 15, 4077–4091, https://doi.org/10.5194/acp-15-4077-2015, 2015.

Rantanen, M., Karpechko, A. Y., Lipponen, A., Nordling, K., Hyvärinen, O., Ruosteenoja, K., Vihma, T., and Laaksonen, A.: The Arctic has warmed nearly four times faster than the globe since 1979, Commun. Earth Environ., 3, 1–10, https://doi.org/10.1038/s43247-022-00498-3, 2022.

Rose, T., Crewell, S., Löhnert, U., and Simmer, C.: A network suitable microwave radiometer for operational monitoring of the cloudy atmosphere, Atmos. Res., 75, 183–200, https://doi.org/10.1016/j.atmosres.2004.12.005, 2005.

Ruske, S., Topping, D. O., Foot, V. E., Kaye, P. H., Stanley, W. R., Crawford, I., Morse, A. P., and Gallagher, M. W.: Evaluation of machine learning algorithms for classification of primary biological aerosol using a new UV-LIF spectrometer, Atmos. Meas. Tech., 10, 695–708, https://doi.org/10.5194/amt-10-695-2017, 2017.

Šantl-Temkiv, T., Lange, R., Beddows, D., Rauter, U., Pilgaard, S., Dall'osto, M., Gunde-Cimerman, N., Massling, A., and Wex, H.: Biogenic Sources of Ice Nucleating Particles at the High Arctic Site Villum Research Station, Environ. Sci. Technol., 53, 10580–10590, https://doi.org/10.1021/acs.est.9b00991, 2019.

Sattler, B., Puxbaum, H., and Psenner, R.: Bacterial growth in supercooled cloud droplets, Geophys. Res. Lett., 28, 239–242, https://doi.org/10.1029/2000GL011684, 2001.

Schmale, J., Zieger, P., and Ekman, A. M.: Aerosols in current and future Arctic climate, Nat. Clim. Change, 11, 95–105, https://doi.org/10.1038/s41558-020-00969-5, 2021.

Sharma, S., Andrews, E., Barrie, L. A., Ogren, J. A., and Lavoué, D.: Variations and sources of the equivalent black carbon in the high Arctic revealed by long-term observations at Alert and Barrow: 1989–2003, J. Geophys. Res.-Atmos., 111, D14208, https://doi.org/10.1029/2005JD006581, 2006.

Shi, Y., Liu, X., Wu, M., Zhao, X., Ke, Z., and Brown, H.: Relative importance of high-latitude local and long-range-transported dust for Arctic ice-nucleating particles and impacts on Arctic mixed-phase clouds, Atmos. Chem. Phys., 22, 2909–2935, https://doi.org/10.5194/acp-22-2909-2022, 2022.

Shingler, T., Dey, S., Sorooshian, A., Brechtel, F. J., Wang, Z., Metcalf, A., Coggon, M., Mülmenstädt, J., Russell, L. M., Jonsson, H. H., and Seinfeld, J. H.: Characterisation and airborne deployment of a new counterflow virtual impactor inlet, Atmos. Meas. Tech., 5, 1259–1269, https://doi.org/10.5194/amt-5-1259-2012, 2012.

Shupe, M. D., Rex, M., Blomquist, B., G. Persson, P. O., Schmale, J., Uttal, T., Althausen, D., Angot, H., Archer, S., Bariteau, L., Beck, I., Bilberry, J., Bucci, S., Buck, C., Boyer, M., Brasseur, Z., Brooks, I. M., Calmer, R., Cassano, J., Castro, V., Chu, D., Costa, D., Cox, C. J., Creamean, J., Crewell, S., Dahlke, S., Damm, E., de Boer, G., Deckelmann, H., Dethloff, K., Dütsch, M., Ebell, K., Ehrlich, A., Ellis, J., Engelmann, R., Fong, A. A., Frey, M. M., Gallagher, M. R., Ganzeveld, L., Gradinger, R., Graeser, J., Greenamyer, V., Griesche, H., Griffiths, S., Hamilton, J., Heinemann, G., Helmig, D., Herber, A., Heuzé, C., Hofer, J., Houchens, T., Howard, D., Inoue, J., Jacobi, H. W., Jaiser, R., Jokinen, T., Jourdan, O., Jozef, G., King, W., Kirchgaessner, A., Klingebiel, M., Krassovski, M., Krumpen, T., Lampert, A., Landing, W., Laurila, T., Lawrence, D., Lonardi, M., Loose, B., Lüpkes, C., Maahn, M., Macke, A., Maslowski, W., Marsay, C., Maturilli, M., Mech, M., Morris, S., Moser, M., Nicolaus, M., Ortega, P., Osborn, J., Pätzold, F., Perovich, D. K., Petäjä, T., Pilz, C., Pirazzini, R., Posman, K., Powers, H., Pratt, K. A., Preußer, A., Quéléver, L., Radenz, M., Rabe, B., Rinke, A., Sachs, T., Schulz, A., Siebert, H., Silva, T., Solomon, A., Sommerfeld, A., Spreen, G., Stephens, M., Stohl, A., Svensson, G., Uin, J., Viegas, J., Voigt, C., von der Gathen, P., Wehner, B., Welker, J. M., Wendisch, M., Werner, M., Xie, Z. Q., and Yue, F.: Overview of the MOSAiC expedition: Atmosphere, Elem. Sci. Anth., 10, 1–54, https://doi.org/10.1525/elementa.2021.00060, 2022.

Si, M., Evoy, E., Yun, J., Xi, Y., Hanna, S. J., Chivulescu, A., Rawlings, K., Veber, D., Platt, A., Kunkel, D., Hoor, P., Sharma, S., Leaitch, W. R., and Bertram, A. K.: Concentrations, composition, and sources of ice-nucleating particles in the Canadian High

Arctic during spring 2016, Atmos. Chem. Phys., 19, 3007–3024, https://doi.org/10.5194/acp-19-3007-2019, 2019.

Sjostrom, D. J. and Welker, J. M.: The influence of air mass source on the seasonal isotopic composition of precipitation, eastern USA, J. Geochem. Expl., 102, 103–112, https://doi.org/10.1016/j.gexplo.2009.03.001, 2009.

Sodemann, H., Schwierz, C., and Wernli, H.: Interannual variability of Greenland winter precipitation sources: Lagrangian moisture diagnostic and North Atlantic Oscillation influence, J. Geophys. Res., 113, D03107, https://doi.org/10.1029/2007JD008503, 2008.

Solomon, A., de Boer, G., Creamean, J. M., McComiskey, A., Shupe, M. D., Maahn, M., and Cox, C.: The relative impact of cloud condensation nuclei and ice nucleating particle concentrations on phase partitioning in Arctic mixed-phase stratocumulus clouds, Atmos. Chem. Phys., 18, 17047–17059, https://doi.org/10.5194/acp-18-17047-2018, 2018.

Spänkuch, D., Hellmuth, O., and Görsdorf, U.: What Is a Cloud? Toward a More Precise Definition, Bull. Am. Meteorol. Soc., 103, E1894–E1929, https://doi.org/10.1175/BAMS-D-21-0032.1, 2022.

Steen-Larsen, H. C., Johnsen, S. J., Masson-Delmotte, V., Stenni, B., Risi, C., Sodemann, H., Balslev-Clausen, D., Blunier, T., Dahl-Jensen, D., Ellehøj, M. D., Falourd, S., Grindsted, A., Gkinis, V., Jouzel, J., Popp, T., Sheldon, S., Simonsen, S. B., Sjolte, J., Steffensen, J. P., Sperlich, P., Sveinbjörnsdóttir, A. E., Vinther, B. M., and White, J. W. C.: Continuous monitoring of summer surface water vapor isotopic composition above the Greenland Ice Sheet, Atmos. Chem. Phys., 13, 4815–4828, https://doi.org/10.5194/acp-13-4815-2013, 2013.

Stein, A. F., Draxler, R. R., Rolph, G. D., Stunder, B. J., Cohen, M. D., and Ngan, F.: Noaa's hysplit atmospheric transport and dispersion modeling system, Bull. Am. Meteorol. Soc., 96, 2059–2077, https://doi.org/10.1175/BAMS-D-14-00110.1, 2015.

Stopelli, E., Conen, F., Morris, C. E., Herrmann, E., Bukowiecki, N., and Alewell, C.: Ice nucleation active particles are efficiently removed by precipitating clouds, Sci. Rep., 5, 16433, https://doi.org/10.1038/srep16433, 2015.

Storelvmo, T.: Aerosol Effects on Climate via Mixed-Phase and Ice Clouds, Ann. Rev. Earth Planet. Sc., 45, 199–222, https://doi.org/10.1146/annurev-earth-060115-012240, 2017.

Sze, K. C. H., Wex, H., Hartmann, M., Skov, H., Massling, A., Villanueva, D., and Stratmann, F.: Ice-nucleating particles in northern Greenland: annual cycles, biological contribution and parameterizations, Atmos. Chem. Phys., 23, 4741–4761, https://doi.org/10.5194/acp-23-4741-2023, 2023.

Szopa, S., Naik, V., Adhikary, B., Artaxo, P., Berntsen, T., Collins, W. D., Aas, W., Akritidis, D., Allen, R. J., Kanaya, Y., Prather, M. J., Kuo, C., Zhai, P., Pirani, A., Connors, S., Péan, C., Berger, S., Caud, N., Chen, Y., Goldfarb, L., Gomis, M., Huang, M., Leitzell, K., Lonnoy, E., Matthews, J., Maycock, T., Waterfield, T., Yelekçi, O., Yu, R., and Zhou, B.: 6 – Short-lived Climate Forcers, Climate Change 2021: The Physical Science Basis. Contribution of Working Group I to the Sixth Assessment Report of the Intergovernmental Panel on Climate Change, 817–922, https://doi.org/10.1017/9781009157896.008, 2021.

Taylor, P. C., Boeke, R. C., Li, Y., and Thompson, D. W. J.: Arctic cloud annual cycle biases in climate models, Atmos. Chem. Phys., 19, 8759–8782, https://doi.org/10.5194/acp-19-8759-2019, 2019.

Tobo, Y., Prenni, A. J., Demott, P. J., Huffman, J. A., McCluskey, C. S., Tian, G., Pöhlker, C., Pöschl, U., and Kreidenweis, S. M.: Biological aerosol particles as a key determinant of ice nuclei populations in a forest ecosystem, J. Geophys. Res.-Atmos., 118, 100–110, https://doi.org/10.1002/jgrd.50801, 2013.

Tobo, Y., Adachi, K., DeMott, P. J., Hill, T. C., Hamilton, D. S., Mahowald, N. M., Nagatsuka, N., Ohata, S., Uetake, J., Kondo, Y., and Koike, M.: Glacially sourced dust as a potentially significant source of ice nucleating particles, Nat. Geosci., 12, 253–258, https://doi.org/10.1038/s41561-019-0314-x, 2019.

Urbański, J. A. and Litwicka, D.: The decline of Svalbard land-fast sea ice extent as a result of climate change, Oceanologia, 64, 535–545, https://doi.org/10.1016/j.oceano.2022.03.008, 2022.

Welker, J. M., Wookey, P. A., Parsons, A. N., Press, M. C., Callaghan, T. V., and Lee, J. A.: Leaf carbon isotope discrimination and vegetative responses of Dryas octopetala to temperature and water manipulations in a High Arctic polar semi-desert, Svalbard, Oecologia, 95, 463–469, https://doi.org/10.1007/BF00317428, 1993.

Wendisch, M., Brückner, M., Crewell, S., Ehrlich, A., Notholt, J., Lüpkes, C., Macke, A., Burrows, J. P., Rinke, A., Quaas, J., Maturilli, M., Schemann, V., Shupe, M. D., Akansu, E. F., Barrientos-Velasco, C., Bärfuss, K., Blechschmidt, A. M., Block, K., Bougoudis, I., Bozem, H., Böckmann, C., Bracher, A., Bresson, H., Bretschneider, L., Buschmann, M., Chechin, D. G., Chylik, J., Dahlke, S., Deneke, H., Dethloff, K., Donth, T., Dorn, W., Dupuy, R., Ebell, K., Egerer, U., Engelmann, R., Eppers, O., Gerdes, R., Gierens, R., Gorodetskaya, I. V., Gottschalk, M., Griesche, H., Gryanik, V. M., Handorf, D., Harm-Altstädter, B., Hartmann, J., Hartmann, M., Heinold, B., Herber, A., Herrmann, H., Heygster, G., Höschel, I., Hofmann, Z., Hölemann, J., Hünerbein, A., Jafariserajehlou, S., Jäkel, E., Jacobi, C., Janout, M., Jansen, F., Jourdan, O., Jurányi, Z., Kalesse-Los, H., Kanzow, T., Käthner, R., Kliesch, L. L., Klingebiel, M., Knudsen, E. M., Kovács, T., Körtke, W., Krampe, D., Kretzschmar, J., Kreyling, D., Kulla, B., Kunkel, D., Lampert, A., Lauer, M., Lelli, L., Von Lerber, A., Linke, O., Löhnert, U., Lonardi, M., Losa, S. N., Losch, M., Maahn, M., Mech, M., Mei, L., Mertes, S., Metzner, E., Mewes, D., Michaelis, J., Mioche, G., Moser, M., Nakoudi, K., Neggers, R., Neuber, R., Nomokonova, T., Oelker, J., Papakonstantinou-Presvelou, I., Pätzold, F., Pefanis, V., Pohl, C., Van Pinxteren, M., Radovan, A., Rhein, M., Rex, M., Richter, A., Risse, N., Ritter, C., Rostosky, P., Rozanov, V. V., Donoso, E. R., Garfias, P. S., Salzmann, M., Schacht, J., Schäfer, M., Schneider, J., Schnierstein, N., Seifert, P., Seo, S., Siebert, H., Soppa, M. A., Spreen, G., Stachlewska, I. S., Stapf, J., Stratmann, F., Tegen, I., Viceto, C., Voigt, C., Vountas, M., Walbröl, A., Walter, M., Wehner, B., Wex, H., Willmes, S., Zanatta, M., and Zeppenfeld, S.: Atmospheric and Surface Processes, and Feedback Mechanisms Determining Arctic Amplification, Bull. Am. Meteorol. Soc., 104, E208–E242, https://doi.org/10.1175/BAMS-D-21-0218.1, 2023.

WMO: Guide to Meteorological Instruments and Methods of Observation – WMO-N O. 8, Secretariat of the World Meteorological Organization, Geneva, Switzerland, World Meteorological Organization, https://library.wmo.int/idurl/4/41650 (last access: 1 March 2023), 2008.

Wookey, R., Robinson AN Parsons Welker, C. J., Press, M., Callaghan, T., Lee, J., Robinson, C., Callaghan MC Press, T., Parsons, A., and Welker, J.: Environmental constraints on the growth, photosynthesis and reproductive development of Dryas octopetala at a high Arctic polar semi-desert, Svalbard, Oecologia, 102, 478–489, 1995.

Xia, Z., Welker, J. M., and Winnick, M. J.: The Seasonality of Deuterium Excess in Non-Polar Precipitation, Global Biogeochem. Cy., 36, 1–31, https://doi.org/10.1029/2021GB007245, 2022.

Zieger, P., Fierz-Schmidhauser, R., Gysel, M., Ström, J., Henne, S., Yttri, K. E., Baltensperger, U., and Weingartner, E.: Effects of relative humidity on aerosol light scattering in the Arctic, Atmos. Chem. Phys., 10, 3875–3890, https://doi.org/10.5194/acp-10-3875-2010, 2010.

Zieger, P., Heslin-Rees, D., Karlsson, L., Koike, M., Modini, R., and Krejci, R.: Black carbon scavenging by low-level Arctic clouds, Nat. Commun., 14, 5488, https://doi.org/10.1038/s41467-023-41221-w, 2023.